

Relativistic strange stars with charged anisotropic matter

S. K. Maurya,^{1,*} Ayan Banerjee,^{2,3,†} and Phongpichit Channuie^{4,‡}

¹*Department of Mathematical and Physical Sciences,
College of Arts and Science, University of Nizwa, Nizwa, Sultanate of Oman.*
²*Astrophysics and Cosmology Research Unit, University of KwaZulu Natal,
Private Bag X54001, Durban 4000, South Africa.*

³*Department of Mathematics, Jadavpur University, Kolkata-700032, India.*

⁴*School of Science, Walailak University,
Nakhon Si Thammarat, 80160 Thailand.*

(Dated: May 23, 2022)

Abstract

In this article we perform a detailed theoretical analysis for a class of new exact solutions with anisotropic fluid distribution of matter for compact objects in hydrostatic equilibrium. To achieve this we call the relation between the metric functions, namely, embedding class one condition. The investigation is carried out by generalising the properties of a spherical star with an emphasis on hydrostatic equilibrium equation, i.e., the generalised Tolman-Oppenheimer-Volkoff equation, in our understanding of these compact objects. We match the interior solution to an exterior Reissner-Nordström solution, and study some physical features of this models, such as the energy conditions, speeds of sound, and mass - radius relation of the star. We also show that obtained solution is compatible with observational data for compact object Her X-1.

PACS numbers:

*Electronic address: sunil@unizwa.edu.om

†Electronic address: ayan7575@yahoo.co.in

‡Electronic address: channuie@gmail.com

I. Introduction

Over the past few decades, an important and intriguing challenge in astrophysics is the study of relativistic compact stars have attracted much attention. On the other hand, another very important issue is the solutions of Einsteins equations for static spherically symmetric gravitational fields with different inputs for the physical content (perfect fluid, dust etc.) and features (anisotropy, charge, rotation, etc.). Among solutions found so far a large section of physicist considered that these objects are composed of a perfect fluid. Following the tradition of calling spherically symmetric star has now changed in the real world, because, strong theoretical evidences suggest that highly dense celestial bodies are not composed purely of perfect fluids. However, in some cases the objects are found with different physical phenomena could give rise to anisotropy (principal stresses unequal).

The first theoretical attempt for considering the anisotropy effect was performed by Rudereman [1]. He argued that at very high densities of the order of 10^{15}g/cm^3 , may have anisotropic features where the nuclear interaction become relativistic in nature. Soon after Bowers and Liang in (1974) [2]- studied anisotropic for static spherically symmetric general relativistic configurations. After the pioneering work by Mak and Harko [3] found the exact solutions of Einstein's gravitational field equations for an anisotropic fluid sphere. The general relativistic analog for anisotropic stars were considered by several authors such as Sharma and Maharaj [4], Rahaman *et al.*, [5], Banerjee *et al.* [6], Matondo and Maharaj [7] and so on. They were successfully used the anisotropy in fluid pressure of a compact relativistic star. A lot of solutions have been developed based on this method up to now [8–13].

The theoretical motivation behind the concept of an embedding general n-dimensional manifold in higher-dimensional spacetime has now an interesting problem that plays the essential role in studying the structure of stars. In particular, the primary motivation of embedding problem comes from the work by Schläfli [14], soon after the publication by Riemann work. He considered the problem of how to locally embed such manifolds in Euclidean space E_N with $N = n(n + 1)/2$. A central aspect of this embedding is not only to search for new solutions, but also search for higher-dimensional generalizations of our known four-dimensional solutions. A few examples in this direction, such as Whitne's embedding theorem [15], stating that any n-dimensional manifold can be embedded in R^n ,

Jannet-Cartan's theorem [16, 17], assert that any real analytic n-dimensional Riemannian manifold can be locally embedded isometrically in $n(n+1)/2$ -dimensional Euclidean space; and the Nash's embedding theorem, which shows that Riemannian manifolds could always be regarded as Riemannian submanifolds, and be isometrically embedded in some Euclidean spaces. More recently, some other embedding theorems have been devoted in the study of braneworld consequences in general relativity. The braneworld models, based on the assumption that four dimensional space-time is a 3-brane (domain wall), embedded in a 5-dimensional Einstein space [18, 19]. This route has been successfully used in the context of astrophysics as well as cosmological study.

On the other hand, it is well known that n dimensional manifold V_n can be embedded in $m = n(n + 1)/2$ dimensions pseudo-Euclidean space, which is called the embedding class of V_n . Inspired by this unification, the embedding 4-dimensional space-time into 5-dimensional flat space-time has been emerged by using the spherical coordinates transformation which is known as embedding class one condition satisfying the Karmakar's condition [20]. In this case, the metric functions are dependent on each other and obtained exact solutions of Einstein's equation reduce to a single-generating function. This method is adopted by various author, in the simple model of spherically symmetric stars with anisotropic pressure [21–23].

However, the discovery of several peculiar compact stellar objects, such as X-ray pulsar Her X-1, X-ray burster 4U 1820-30, X-ray sources 4U 1728-34, PSR 0943+10, millisecond pulsar SAX J 1808.4-3658, and RX J185635-3754 provoked us to rethink the commonly accepted scenario for stellar model. In other words, the characteristic nature of such compact objects are still unknown to us. More recently, some attempted models to explain compact objects often based on various inputs including charged, uncharged with different EOS [24–33]. The aim of the present paper is to obtain a new class of solutions for charged fluid sphere, using the embedding class one conditions. It is found that these models can accommodate a compact stellar object Her X-1, given in Gangopadhyay *et al* [34].

The paper is structured as follows: In Sec. II, we proposed class one condition and the metric functions related in a closed form by using class one condition. In section III, we set up the relevant field equations and its solutions for charged fluid distribution. In Sec. IV, we derived an exact solution of the EinsteinMaxwell equations by assuming a simplest form of an electric field E . In next, we presented physical analysis of stellar models with

the observational stellar mass for Her X-1 and discuss the stability of the charged stars by employing modified TOV equations in Sec. V. We summarise the results obtained in this paper in Sec. VI.

II. Embedding class one condition for spherical symmetric line element:

The most general form of line element that describe a static fluid distribution with spherical symmetry, is given in terms of $x^i = (r, \theta, \phi, t)$ as follows:

$$ds^2 = e^{\nu(r)} dt^2 - e^{\lambda(r)} dr^2 - r^2(d\theta^2 + \sin^2 \theta d\phi^2), \quad (1)$$

where the unknowns $\nu(r)$ and $\lambda(r)$ are both metric functions, which yet to be determined by solving the Einstein field equations.

The influence of determining the class one condition of the above metric (1), we suppose 5-dimensional flat line element as

$$ds^2 = - (dx^1)^2 - (dx^2)^2 - (dx^3)^2 - (dx^4)^2 + (dx^5)^2, \quad (2)$$

here we have transformed the coordinate system via the following rescaling:

$$\begin{aligned} x^1 &= r \sin \theta \cos \phi, & x^2 &= r \sin \theta \sin \phi, & x^3 &= r \cos \theta, & x^4 &= \sqrt{K} e^{\frac{\nu}{2}} \cosh \frac{t}{\sqrt{K}}, \\ x^5 &= \sqrt{K} e^{\frac{\nu}{2}} \sinh \frac{t}{\sqrt{K}}, \end{aligned}$$

where K is a positive constant. Now, using the above transformation, one can derive the following expression for the above metric which is

$$ds^2 = e^{\nu(r)} dt^2 - \left(1 + \frac{K e^{\nu}}{4} \nu'^2 \right) dr^2 - r^2 (d\theta^2 + \sin^2 \theta d\phi^2), \quad (3)$$

which reduce to a four dimensional spherically symmetric line element. This metric describes a 5-D pseudo-Euclidean space embedded in a (3+1)-dimensional spacetime. Now, comparing the Eqs. 1 and 3, one can obtain the following relations

$$e^{\lambda} = \left(1 + \frac{K e^{\nu}}{4} \nu'^2 \right). \quad (4)$$

It is worthwhile to mention that the Eq. (4) provides the embedding class condition (we will refer our readers for more details in Ref. [20, 21]).

III. The Einstein-Maxwell Field Equations for Charged Matter Distribution with anisotropic pressure

For completeness we start by writing the Einstein-Maxwell field equations are the well known expressions on a four dimensional space-time manifold, reads

$$R^\mu_\varphi - \frac{1}{2} R g^\mu_\varphi = -8\pi(T^\mu_\varphi + E^\mu_\varphi), \quad (5)$$

where $\kappa = 8\pi$ is the Einstein coupling constant. We use geometrized units $G = c = 1$ with G and c are being the Newtonian gravitational constant and speed of photons in vacuum, respectively.

In the considered spacetime the energy-momentum tensor include the terms from the Maxwell's equation and the complete form of anisotropic charged fluid matter is given by

$$T_\mu\varphi = [(\rho + p_t)u^\mu u_\varphi - p_t\delta^\mu_\varphi + (p_r - p_t)\chi^\mu\chi_\varphi] + \frac{1}{4\pi} \left[F^{\mu k}F_{\mu k} - \frac{1}{4}\delta^\mu_\varphi F^{kl}F_{kl} \right], \quad (6)$$

where u_φ , χ_φ and δ^μ_φ stand for 4-velocity of the fluid, the radial unit vector and the metric tensor respectively. As we know that the 4-velocity and the radial unit vector satisfy the following the conditions:

$$u^\varphi u_\varphi = -1, \quad \chi^\varphi \chi_\varphi = 1 \quad \chi_\varphi u^\varphi = 0. \quad (7)$$

However, the other components (radial and spherical) of the 4-vector are absent. For the considered energy-momentum tensor, the function ρ is the energy density, p_r is the radial pressure and the tangential pressure is denoted by p_t , respectively. It is worth noting that the components for T^μ_φ and E^μ_φ are defined as follows:

$$T^1_1 = -p_r, \quad T^2_2 = T^3_3 = -p_t, \quad T^4_4 = \rho \quad (8)$$

$$E^1_1 = -E^2_2 = -E^3_3 = E^4_4 = \frac{1}{8\pi} e^{\nu+\lambda} F^{14} F^{41}. \quad (9)$$

Now, the Maxwell's electromagnetic field equations provides the following relationships

$$[\sqrt{-g}F^{\mu\varphi}]_{,\varphi} = 4\pi j^\mu \sqrt{-g}, \quad (10)$$

where j^μ is the four-current density. For the choice of the electromagnetic field only non vanishing components of the electromagnetic field tensor are F^{01} and F^{10} due to charge, and are related by $F^{01} = -F^{10}$. The Maxwell electromagnetic tensor, $F^{\mu\varphi}$, can be written

in terms of four-potential A^μ : $F_{\mu\varphi} = A_{\mu,\varphi} - A_{\varphi,\mu}$. So, for non vanishing field tensor, only the existing potential is $A_0 = \phi$. In addition, the potential has considered as a spherical symmetry, i.e., $\phi = \phi(r)$. Now using the Eq. (10) one can obtain for the electric field as

$$F^{01}(r) = E(r) = e^{-(\nu+\lambda)/2} r^{-2} \int_0^r 4\pi j^0 e^{(\nu+\lambda)/2} dr'. \quad (11)$$

Let us consider the total charge inside a sphere of radial coordinate r , is $q(r)$ and it follows

$$q(r) = \int_0^r 4\pi j^0 r'^2 e^{(\nu+\lambda)/2} dr', \quad (12)$$

Finally, using the Eq. (11) and (12) we obtain the expression for electric field is

$$E(r) = e^{-(\nu+\lambda)/2} r^{-2} q(r). \quad (13)$$

After accomplishing the effects due to the electric field and pressure anisotropy, the Einstein-Maxwell field equations with the metric (1) provides the following relationships

$$8\pi\rho(r) = \frac{K e^\nu \nu' [4r(2\nu'' + \nu'^2) + \nu'(4 + K\nu'^2 e^\nu)]}{r^2 (4 + K\nu'^2 e^\nu)^2} - \frac{q^2}{r^4}, \quad (14)$$

$$8\pi p_r(r) = \frac{\nu' (4r - K\nu' e^\nu)}{r^2 (4 + K\nu'^2 e^\nu)} + \frac{q^2}{r^4}, \quad (15)$$

$$8\pi p_t(r) = \left[\frac{2\nu' (4 + K\nu'^2 e^\nu) - 2(K\nu' e^\nu - 2r)(2\nu'' + \nu'^2)}{r (4 + K\nu'^2 e^\nu)^2} \right] - \frac{q^2}{r^4}. \quad (16)$$

where primes denote differentiation with respect to the radial coordinate r . The solution for the potential metric $e^{-\lambda(r)}$ is given by

$$e^{-\lambda(r)} = 1 - \frac{2m(r)}{r} + \frac{q^2}{r^2}, \quad (17)$$

where, the parameters q and m represent the charge and mass within the radius r . In the present case, considering the Eq. (15) and (16), one may expressed in the following equivalent form

$$8\pi\Delta + \frac{2q^2}{r^4} = + (K\nu' e^\nu - 2r) \left[\frac{\nu' (4 + K\nu'^2 e^\nu) - 2r(2\nu'' + \nu'^2)}{r^2 (4 + K\nu'^2 e^\nu)^2} \right], \quad (18)$$

where $\Delta = p_t - p_r$ is denoted as the anisotropy factor, and it's measure the pressure anisotropy of the fluid. It is important to note that $\Delta = 0$ at the origin, $r = 0$, corresponds to the particular case of an isotropic pressure. The factor Δ/r represents a force due to the anisotropic nature of the fluid. The anisotropy will be repulsive or directed outwards if $p_t > p_r$, and attractive or directed inward when $p_t < p_r$.

It is clear from the Eqs. (14-16), that we have six unknowns, namely, $\rho(r)$, $p_r(r)$, $p_t(r)$, $\nu(r)$, $\lambda(r)$ and $q^2(r)$, with three independent equations. In attempting to find an exact solutions, it is difficult due to the nonlinearity of the differential equations. Therefore, there are two degrees of freedom and one can adopt different approaches i.e., by choosing a specific choice for a physically reasonable mass function $m(r)$, by specifying an EOS of the form $p = p(\rho)$, or by established a relation between gravitational potentials ν and λ based on physical grounds in this case of charged fluid.

In order to obtain a unique solution we consider embedding class one conditions that relates a close connection between two metric functions as discussed in Section I, for the electrically charged fluid sphere. Some recent treatments have been considered in Ref. [35–37], where they studied compact objects with anisotropic pressure via embedding.

IV. Generalized charged anisotropic solution for compact star

In this model we will address the solutions for charged fluid model by adopting a single generic function $\lambda(r)$. The ansatz has a geometric interpretation from physical point of view and was previously used to obtain solutions for compact stellar objects [38–40]. However, in this article we are interested in another aspect of the problem, mainly the solution that can be used to model for compact object Her X-1.

The system we study here is characterized by the fact that $\lambda(0) = \text{finite constant}$ for charged compact star and energy density $\rho(r)$, radial pressure $p_r(r)$, and tangential pressure $p_t(r)$ should be finite at the origin. For a physically meaningful solution, we should retain as much of standard physics as possible, i.e., the electric field at the centre is zero and $m(0) = 0$ with $m'(r) > 0$. Let us now suppose the generic function $\lambda = \lambda(r)$ with the following expression

$$\lambda(r) = \ln\left(1 + a r^2 (1 + b r^2)^{2n}\right). \quad (19)$$

In this particular approach, we keep in mind that $\lambda'(r) = 0$ and $\lambda''(r) > 0$. Now, substituting the value of λ into the Eq. (4), we obtain

$$\nu(r) = 2 \ln[A + B (1 + b r^2)^{1+n}], \quad (20)$$

where A is integration constant and $B = \sqrt{a} / \left(4 b \sqrt{K} (n + 1)\right)$. Notably, the resulting metric function $\nu(0) = 2 \ln(A + B)$, $\nu'(r) = \frac{4 r b B (n+1) (1+b r^2)^n}{[A+B(1+b r^2)^{n+1}]}$ and $\nu''(r) =$

$\frac{4(n+1)bB(1+br^2)^{n-1}[A(1+br^2+2nb^2)-B(1+br^2)^n(b^2r^4-1)]}{[A+B(1+br^2)^{1+n}]^2}$. The aforesaid decompositions clearly implies that $\nu(0) > 0$, $\nu'(0) = 0$ and $\nu''(0) = \frac{4(n+1)bB}{(A+B)} > 0$, which provides $(A+B) > 0$. The motivation behind the particular choice of metric function (19), is not new in stellar modelling. Similar forms for the metric function has earlier been considered by Singh *et al.* [31] and Maurya *et al.* [36] for positive and negative power of n for anisotropic matter distribution using the embedding classone condition.

To explore the physical content, the parameter n plays an important role in determining the structure and stability of the compact object. Here, we will consider the following three cases (i) when $n > 0$ and $b > 0$, (ii) when $n > 0$ and $b > 0$, and (iii) when $-1 \leq n < 0$ and $b \in \mathbb{R}$. The choice of the range of free parameters are a reasonable assumption in the sense that it admits physically viable models and nature of the matter content the star. In the relativistic regime, we describe here the stellar compact objects such as Her X-1, which justifies the choice of parameter for charged anisotropic fluids sphere.

Furthermore, we assume some simplest form of an electric field intensity E within the radius r , is given by

$$E^2 = \frac{q^2}{r^4} = q_0 a^2 r^4 (1 + br^2)^{2n}, \quad (21)$$

where q_0 is positive constant. The expression is invariant under the transformation $E \rightarrow -E$, and deal with the positive square root of E^2 . Note that the electric field E vanishes at the centre i.e., $r=0$, to construct viable stellar models. In doing so, we proceed from the assumption that our configuration consisting of charged relativistic object, with anisotropic matter distribution. Making use of this expression, we obtain the mass function using the Eq. (17), which yield

$$m(r) = \frac{r}{2} \left[\frac{a r^2 (1 + br^2)^{2n}}{[1 + a r^2 (1 + br^2)^{2n}]} + q_0 a^2 r^6 (1 + br^2)^{2n} \right]. \quad (22)$$

It is interesting to observe that $m(0) = 0$ at the centre. However, both $q(r)$ and $m(r)$ are positive when $r > 0$ for all the above three cases of n . This indicate that $q(r)$ and $m(r)$ are increasing monotonically away from centre and attain regular minima at $r = 0$.

We now determine the Einstein-Maxwell system of Eqs. (14)-(16) for charged anisotropic

matter with the line element (1), reduces to the following equations:

$$\rho(r) = -\frac{q_0 a^2 x^2 \Psi^{2n}}{8\pi} + \frac{1}{8\pi} \left[\frac{a \Psi^{2n}}{(1+a x \Psi^{2n})} + \frac{2 a \Psi^{2n-1} (\Psi + 2 n x)}{(1+a x \Psi^{2n})^2} \right], \quad (23)$$

$$p_r(r) = \frac{q_0 a^2 x^2 \Psi^{2n}}{8\pi} + \frac{1}{8\pi} \left[\frac{4 b B (1+n) \Psi^n}{(1+a x \Psi^{2n}) (A+B \Psi^{1+n})} - \frac{a \Psi^{2n}}{(1+a x \Psi^{2n})} \right], \quad (24)$$

$$p_t(r) = -\frac{q_0 a^2 x^2 \Psi^{2n}}{8\pi} + \frac{\Psi^{n-1}}{8\pi} \left[\frac{4 b B (1+n) (\Psi + b n x) (1+a x \Psi^{2n}) - a \Phi(x)}{(1+a x \Psi^{2n})^2 (A+B \Psi^{1+n})} \right], \quad (25)$$

where $\Psi = (1+b x)^n$ with a , b , and n are arbitrary constants within specific range.

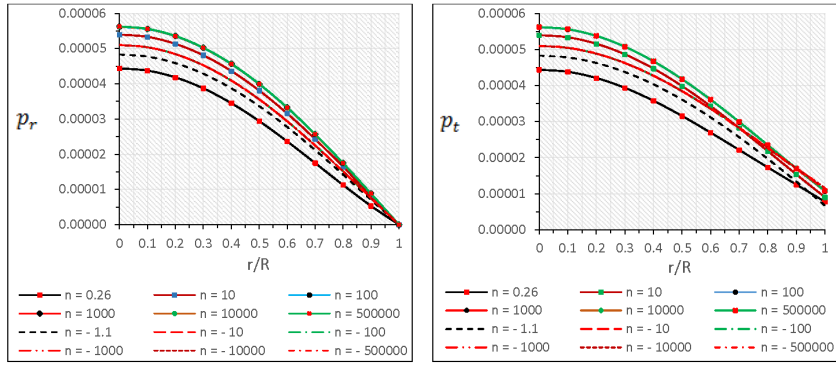


FIG. 1: Behavior of radial pressure (p_r) and tangential pressure (p_t) verses fractional radius r/R for Her X-1. The numerical values of the constants are given in tables 1 & 2.

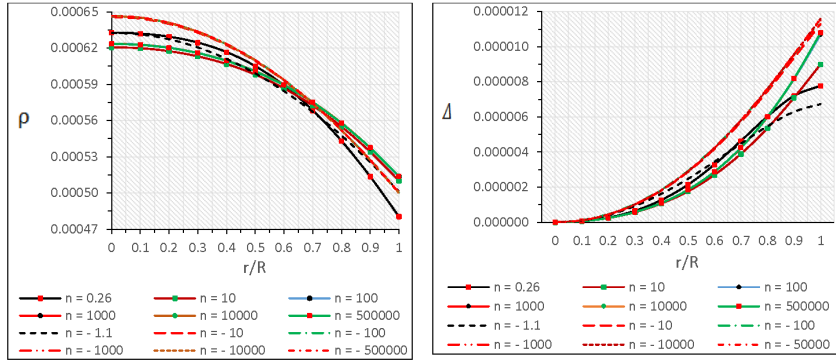


FIG. 2: Behavior of energy density (ρ) and anisotropy factor (Δ) verses fractional radius r/R for Her X-1. The numerical values of the constants are given in tables 1 & 2.

Let us focus on the effect of pressure anisotropy by a term $\Delta = p_t - p_r$, which is defined by

$$\Delta = -\frac{q_0 a^2 x^2 \Psi^{2n}}{4\pi} + \frac{x \Psi^{n-1} (-2 b n + a \Psi^{2n} + a b x \Psi^{2n}) \Delta_1(r)}{8\pi (1+a x \Psi^{2n})^2 (A+B \Psi^{1+n})}, \quad (26)$$

TABLE I: Numerical values of physical parameters when n is positive and mass $M = 0.85 (M_{\odot})$, radius $R = 8.10$ (km) [34].

n	a	b	q_0	A	B	K
0.26	0.005302	0.008	0.0007396	0.6317681	0.11961	2.2796×10^2
10	0.005200	0.000201	0.0002410	0.1929809	0.553565	2.1695×10^2
10	0.005200	0.000201	0.0002410	0.1929809	0.553565	2.1695×10^2
100	0.005225	0.00002016	0.00008999	0.1377625	0.606989	2.1378×10^2
1000	0.0052245	0.000002016	0.00008598	0.1322219	0.612510	2.1372×10^2
500000	0.0052246	0.000000004032	0.00008444	0.1315549	0.613166	2.1370×10^2

where we have considered

$$\Phi(x) = \Psi^n (\Psi + 2n b x) [A + B \Psi^n (1 + 3b x + 2n b x)], \text{ and}$$

$$\Delta_1(x) = [a \Psi^n (A + B \Psi^n) - b B (2 + 2n - a x \Psi^{2n})],$$

which represents a force that arise due to the anisotropic nature of the fluid and it maintain the stability and equilibrium configuration of a stellar stricture, as we will focus later.

Let us emphasize again the behavior of the energy density and pressures for the X-ray pulsar Her X-1 with graphical representation. The variation of pressure and density with radial distance are drawn by using Eqs. (23-25) which are shown in Figs.(1)-(2), respectively. We have used the data set for model parameters given in Table 1 & 2. In this case one can see that energy density is positive and the radial pressure p_r vanish at the boundary of the star for different values of n within the above mentioned specific range .

V. Physical features and Comparative study of the physical parameters for compact star model

In the present section, we will investigate the properties of high density stars based on the obtained solution and the internal structure of stars must satisfy some general physical requirements i.e., energy conditions, hydrostatic stability, checking the speed of sound and to determine the maximum mass of compact objects by analytically expression along with graphical representations. In this view, we model a compact star composed of anisotropic matter, which is useful to describe compact stars like Her X-1.

TABLE II: Numerical values of physical parameters when n is negative and mass $M = 0.85 (M_\odot)$, radius $R = 8.10$ (km) [34].

n	a	b	q_0	A	B	K
-1.1	0.0053	-0.00152	0.00049173	-7.278674	8.027761	2.22474×10^2
-10	0.00541	-0.0001683	0.000241	-0.078002	0.823826	2.17146×10^2
-100	0.0054175	-0.00001683	0.000234	-0.0039761	0.749693	2.17007×10^2
-1000	0.005418	-0.000001683	0.0002332	0.00272656	0.7429889	2.16998×10^2
-10000	0.0054185	-0.0000001683	0.00023181	0.0032851	0.7424096	2.16965×10^8
-500000	0.0054188	-0.000000003366	0.000230444	0.00327454	0.7424053	2.16937×10^{10}

A. Boundary Conditions

To study a static spherically symmetric charged star, we match the interior spacetime to an exterior vacuum Reissner-Nordström spacetime at the junction surface with radius $r = R$, and given by

$$ds^2 = \left(1 - \frac{2M}{r} + \frac{q^2}{r^2}\right) dt^2 - \left(1 - \frac{2M}{r} + \frac{q^2}{r^2}\right)^{-1} dr^2 - r^2(d\theta^2 + \sin^2 \theta d\phi^2), \quad (27)$$

where M denote the total mass of the compact star. We consider the standard matter to be a spherically symmetric anisotropic fluid where the radial pressure p_r must be finite and positive inside the star, and it must vanishes at the boundary $r = R$ of the star [41]. Thus, radial pressure $p_r(R) = 0$, now gives

$$\frac{A}{B} = -\frac{a(1+bR^2)^{2n}[-1+aq_0R^4+a^2q_0R^4(1+bR^2)^{2n}]+F_1(R)}{a(1+bR^2)^n[-1+aq_0R^4+a^2q_0R^6(1+bR^2)^{2n}]}, \quad (28)$$

where $F_1(R) = b(4+4n-aR^2(1+bR^2)^{2n}+a^2q_0R^6(1+bR^2)^{2n}+a^3q_0R^8(1+bR^2)^{2n})$.

We can consider the continuity of the first fundamental form across a surface at $r = R$, implies that $g_{tt}^+ = g_{tt}^-$ and using the condition $e^{-\lambda(R)} = e^{\nu(R)}$ gives

$$B = \frac{1}{\left[\frac{A}{B} + (1+bR^2)^{1+n} \sqrt{1+aR^2(1+bR^2)^{2n}}\right]}. \quad (29)$$

Therefore, one can easily get the total mass of the star for the static case when $e^{-\lambda(R)} = 1 - \frac{2M}{R} + \frac{Q^2}{R^2}$, is given by

$$M(R) = \frac{R}{2} \left[\frac{aR^2(1+bR^2)^{2n} + q_0a^2R^6(1+bR^2)^{2n}[1+aR^2(1+bR^2)^{2n}]}{[1+aR^2(1+bR^2)^{2n}]} \right] \quad (30)$$

We should also note that in the relativistic limit the mass-radius ratio is an important source of information and classification criterion for compact objects [50].

B. Energy conditions

Based on the model under investigation let us carry out the energy conditions within the framework of GR in the interior of the star. Now, considering the usual definition of this energy condition for anisotropic fluids, we examine (i) Null energy condition (NEC), (ii) Weak energy condition (WEC) and (iii) Strong energy condition (SEC), at all points in an interior of a star holds simultaneously. More precisely, we have the following proposition:

$$\mathbf{NEC:} \rho + \frac{E^2}{8\pi} \geq 0, \quad (31)$$

$$\mathbf{WEC}_r: \rho + p_r \geq 0, \quad (32)$$

$$\mathbf{WEC}_t: \rho + p_t + \frac{E^2}{8\pi} \geq 0, \quad (33)$$

$$\mathbf{SEC:} \rho + p_r + 2p_t + \frac{E^2}{4\pi} \geq 0. \quad (34)$$

Using the above expression for all the terms in this inequality, one can easily justify the nature of energy condition for the specific stellar configuration Her X-1. By using the graphical representation, the principle of energy conditions, have been shown in Fig. 3. For the complicated expression given in equations (31-34), we only write down the inequalities and plotted the graphs as a function of the radius. As a result, this is eminently clear from Fig. 3, that all the energy conditions are satisfied for our proposed model.

C. Equilibrium condition

We will now proceed further by investigating hydrostatic equilibrium for different forces acting on it, namely gravitational, hydrostatic, anisotropic and electric forces, respectively. Hence in the present approach we focus on the generalized Tolman-Oppenheimer-Volkoff (TOV) equation [42, 43], and it is given by

$$-\frac{M_G(\rho + p_r)}{r^2} e^{\frac{\lambda-\nu}{2}} - \frac{dp}{dr} + \sigma e^{\frac{\lambda}{2}} \frac{q}{r^2} + \frac{2\Delta}{r} = 0, \quad (35)$$

where the effective gravitational mass $M_G(r)$ is defined by

$$M_G(r) = \frac{1}{2} r^2 \nu' e^{(\nu-\lambda)/2}. \quad (36)$$

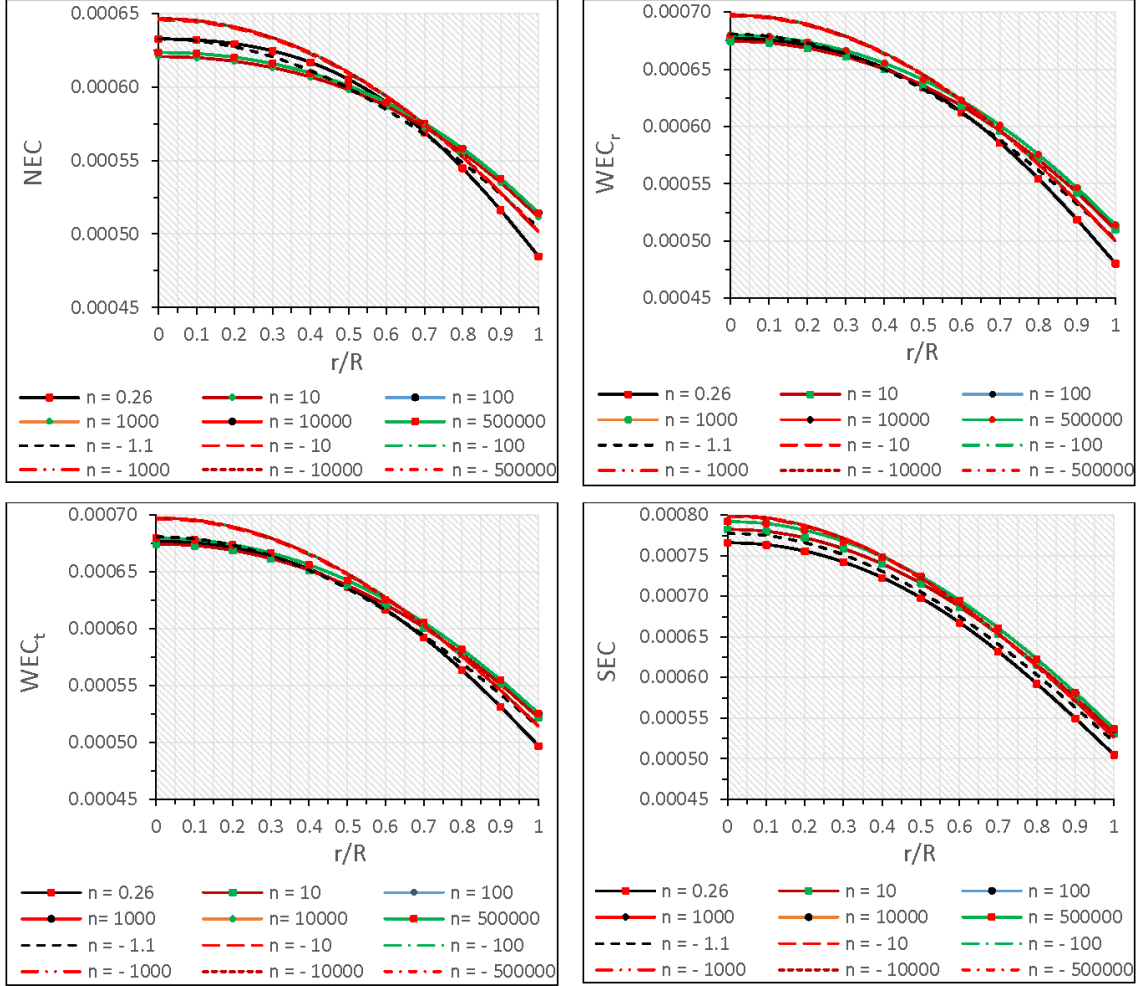


FIG. 3: Behavior of energy conditions versus fractional radius r/R for Her X-1. The numerical values of the constants are given in tables 1 & 2.

Now, using the expression for $M_G(r)$ in Eq. (35), we have

$$-\frac{\nu'}{2}(\rho + p_r) - \frac{dp}{dr} + \sigma \frac{q}{r^2} e^{\frac{\lambda}{2}} + \frac{2\Delta}{r} = 0, \quad (37)$$

Interestingly, the above Eq. (37) may be express as a sum of different components of forces, namely, gravitational forces ($F_g = -\nu'(\rho + p_r)/2$), hydrostatic ($F_h = -dp_r/dr$), electric ($F_e = \sigma q e^{\frac{\lambda}{2}}/r^2$) and anisotropic ($F_a = 2\Delta/r$) forces, respectively. Plugging the typical values from Eqs. (23-25), and using the above expressions, we get straight-forwardly the

different forces, which leads to

$$\begin{aligned}
F_g(r) &= -\frac{b r (n+1) B \Psi^{2n}}{\pi [A + B \Psi^{n+1}]} \left[\frac{a B \Psi^{2n} (1 + 3 b x + 4 n b x) + F_{g1}(x)}{2 [1 + a x \Psi^{2n}]^2 (A + B \Psi^{n+1})} \right], \\
F_h(r) &= \frac{r}{\pi} \left[\frac{[B F_{h1}(x) + A F_{h2}(x)]}{(1 + a x \Psi^{2n})^2 (A + B \Psi^{1+n})^2} - \frac{a F_{h3}(x)}{4(1 + a x \Psi^{2n})^2} - \frac{q_0 a^2 x (\Psi + n b x)}{2 \Psi^{1-2n}} \right], \\
F_e(r) &= \frac{q_0 a^2 r^3 \Psi^n [2 \Psi^n + n b x \Psi^{n-1}]}{2 \pi}, \\
F_a(r) &= \frac{r}{4 \pi} \left[\frac{-q_0 a^2 x \Psi^{2n}}{2} + \frac{\Psi^{n-1} (-2 b n + a \Psi^{2n} + a b x \Psi^{2n}) F_{a1}(x)}{4 (1 + a x \Psi^{2n})^2 (A + B \Psi^{1+n})} \right], \tag{38}
\end{aligned}$$

where for notational convention and make the expression simplicity we use

$$\begin{aligned}
F_{g1}(x) &= 2 b B (n+1) + a A \Psi^{n-1} (1 + b x + 2 n b x), \\
F_{h1}(x) &= b B (n+1) \Psi^{2n} [a \Psi^{2n} + b (1 + 2 a (n+1) x \Psi^{2n})], \\
F_{h2}(x) &= b B (n+1) \Psi^{n-1} [a \Psi^{2n} + b (a x \Psi^{2n} + n (-1 + a x \Psi^{2n}))], \\
F_{h3}(x) &= \Psi^{2n-1} (-2 b n + a \Psi^{2n} + a b x \Psi^{2n}), \\
F_{a1}(x) &= [a \Psi^n (A + B \Psi^n) - b B (2 + 2 n - a x \Psi^{2n})].
\end{aligned}$$

Thus combining the results, which gives a simple expression, as

$$F_g + F_h + F_e + F_a = 0. \tag{39}$$

It is observable that due to the structure of obtained modified TOV equation, the configuration is in static equilibrium under four different forces. As we see from Fig. 4, that all four forces maintain to attain overall equilibrium situation for positive as well as negative values of n . It is to be noted that the electric force seems has negligible effect in this balancing mechanism.

D. Stability Analysis

At this stage we start by assuming a quantity $c^2 = dp/d\rho$, which can be interpreted as a speed of sound propagation. The motivation behind such a construction is to study the stability of the configuration. It is also to be noted that negative c^2 is usually interpreted as an instability, while $c^2 > 1$ indicates superluminal speed of sound. Our aim in the sequel is to confirm that sound speed does not exceed the speed of light, i.e., $0 \leq c^2 < 1$. Here, we shall investigate the speed of sound for charged anisotropic fluid distribution should satisfy the bounds $0 < v_r^2 = dp_r/d\rho < 1$ and $0 < v_t^2 = dp_t/d\rho < 1$, as in Ref. [53]. The velocity of

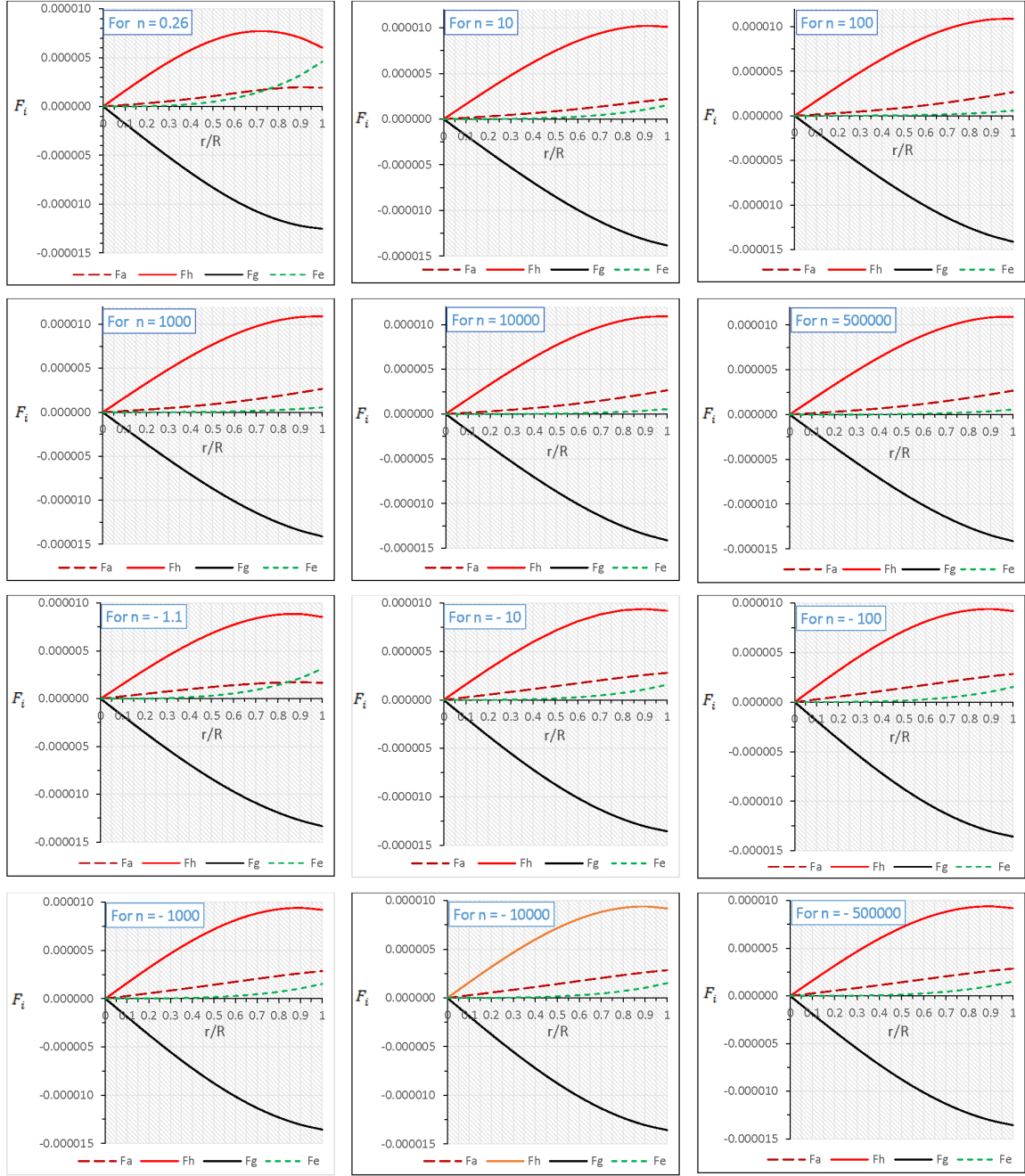


FIG. 4: Behavior of different forces F_i verses fractional radius r/R for Her X-1. The numerical values of the constants are given in tables 1 & 2.

sound alone radial and transverse direction are given by

$$\begin{aligned}
 v_r^2 &= \frac{f_1(x)}{f_2^2(x)} \left[\frac{B v_1(x) + A v_2(x) + a v_3(x) f_2^2(x) - 2 q_0 a^2 f_2^2(x) v_4(x)}{a \Psi^{2n-2} [a v_5(x) + b^2 x v_6(x)] + 2 q_0 a^2 v_4(x)} \right], \\
 v_t^2 &= \frac{\Psi^{n-2}}{f_2^2(x)} \left[\frac{v_8(x) + v_9(x) + v_{10}(x) + v_{11}(x) + b f_1(x) f_2(x) v_{12}(x) + v_{13}(x)}{-a \Psi^{2n-2} [a v_5(x) + b^2 x v_6(x)] + 2 q_0 a^2 v_4(x)} \right]. \quad (40)
 \end{aligned}$$

where the unknown quantity stands for

$$\begin{aligned}
f_1(x) &= (1 + a x \Psi^{2n}), \quad f_2(x) = (A + B \Psi^{n+1}), \\
v_1(x) &= 4 b B (n + 1) \Psi^{2n} [a \Psi^{2n} + b (1 + 2 a (n + 1) x f_1(x))], \\
v_2(x) &= 4 b B (n + 1) \Psi^{n-1} [a \Psi^{2n} + b (a x \psi^{2n} + n (-1 + a x \Psi^{2n}))], \\
v_3(x) &= \Psi^{2n-1} (-2 b n + a \Psi^{2n} + a b x \Psi^{2n}), \quad v_4(x) = x \Psi^{2n-1} (\Psi + b n x) f_1^2(x), \\
v_5(x) &= \Psi^{2n} (5 + a x \Psi^{2n}) + 2 b [a x \Psi^{2n} (5 + a x \Psi^{2n}) + n (-5 + 3 a x \Psi^{2n})], \\
v_6(x) &= [8 n^2 (-1 + a x \Psi^{2n}) + a x \Psi^{2n} (5 + a x \Psi^{2n}) + 2 n (-3 + 5 a x \Psi^{2n})], \\
v_7(x) &= b (4 B (n + 1) - a A (1 + 2 n) x \Psi^n + b^2 B x (4 + 8 n + 4 n^2 + a x \Psi^{2n})), \\
v_8(x) &= -b B (n + 1) \Psi^{n+1} f_1(x) [-a \Psi^n (A + B \Psi^n) + v_7(x)], \\
v_9(x) &= b (n - 1) f_1(x) f_2(x) [-a \psi^n (A + B \Psi^n) + v_7(x)], \\
v_{10}(x) &= -2 a \Psi^{2n} f_2(x) (\Psi + 2 b n x) [-a \Psi^n (A + B \Psi^n) + v_7(x)], \\
v_{11}(x) &= b [-a A (1 + 3 n + 2 n^2) x \Psi^n + 2 B (2 + 4 n + 2 n^2 + a x \Psi^{2n})], \\
v_{12}(x) &= [-a \Psi^n (A + 3 A n + 2 B n \Psi^n) + 2 b^2 B (1 + n) x (2 + 2 n + a x \Psi^{2n}) + v_{11}(x)], \\
v_{13}(x) &= 2 q_0 x a^2 f_1^3(x) f_2^2(x) \Psi^{n+1} (\Psi + b n x).
\end{aligned}$$

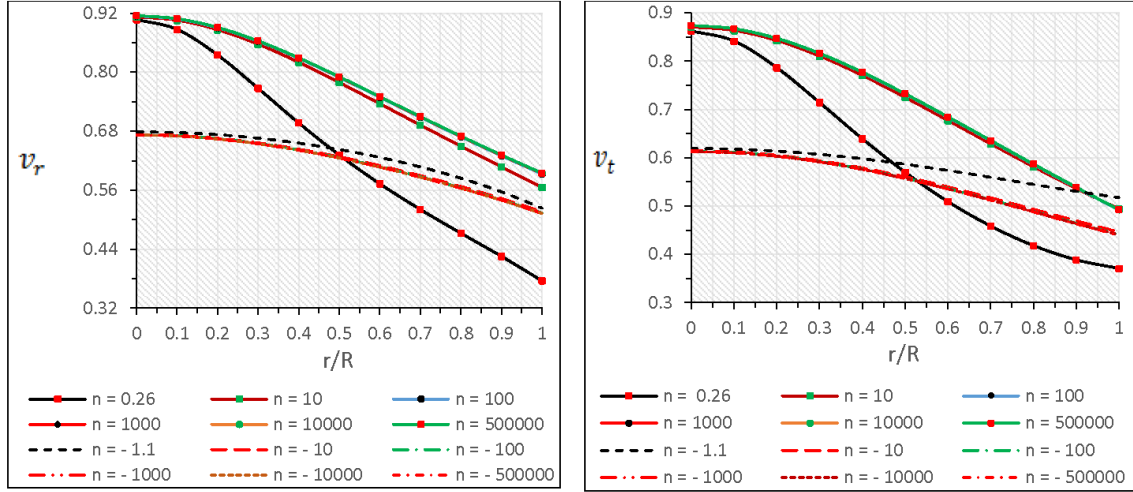


FIG. 5: Behavior of radial velocity (v_r) and tangential velocity (v_t) verses fractional radius r/R for Her X-1. The numerical values of the constants are given in tables 1 & 2.

We present our results in Fig. 5 due to complexity of the expression. According to the graph of the radial/transverse pressures vs. radius, it is interesting to note that both $v_r^2, v_t^2 <$

1 and decreases monotonically from the centre of the star towards the surface of the star. Moreover, both the velocities are positive and finite at the interior of the star Her X-1.

E. Electric charge

Our aim here is to explore the physics governing of the structure of stars includes the charge has affected the structure and stability of strange stars. With that purpose we use graphical representation given in Fig. 6. It is clear from Fig. 6, and Table III & IV, that the charge profile is zero at the center corresponding to vanishing electric field and monotonically increasing away from the center, acquiring a maximum value at the boundary of the star. This implies that the surface of the charged body is more stable than the inner core. We further note that the charge decreases monotonically with an increase on $|n|$ with the difference becoming indistinguishable at the stellar surface for very large values of $|n|$. According to Ref. [36], we can interpret n as a “stabilizing factor”. It can be found by searching for the condition that higher charge configuration reached for large radius and the larger value of the metric coefficient e^λ . From this we understand that the matter and charge are inter-related to each other and the relations are strongly coupled. As mentioned in Ref. [36], the onset of collapse of such a body could proceed in an anisotropic manner or the collapse could lead to the cracking of the object thus avoiding the formation of a black hole.

As pointed out by Ray *et. al.* [44], the charge can be as high as 10^{20} Coulombs (C) and hydrostatic equilibrium may still be achieved. However these equilibrium states are unstable. Bekenstein [45] argued that high charge densities will generate very intense electric fields. If this is that case pair production may be induced within the star and thus destabilize the core. To be more concrete, we calculate the amount of charge at the boundary in units of coulombs for the compact star Her X-1 as follows: (i-1) 8.0760×10^{19} C for $n = 0.26$, (ii-1) 4.6186×10^{19} Coulomb for $n = 10$, (iii-1) 2.8391×10^{19} C for $n = 100$, (iv-1) 2.7752×10^{19} C for $n = 1000$, (v-1) 2.7592×10^{19} C for $n = 10000$, (vi-1) 2.7503×10^{19} C for $n = 500000$ and (i-2) 6.6211×10^{19} C for $n = -1.1$, (ii-2) 0.4710×10^{19} C for $n = -10$, (iii-2) 4.6450×10^{19} C for $n = -100$, (iv-2) 4.6373×10^{19} C for $n = -1000$, (v-2) 4.6238×10^{19} C for $n = -10000$, (vi-2) 4.6104×10^{19} C for $n = -500000$. Here, the amount of charge in coulomb unit throughout the star can be determined by multiplying any recorded value in Table III & IV

TABLE III: The electric charge for compact star Her X-1 for different positive values of n in Km.

r/a	$n = 0.26$	$n = 10$	$n = 100$	$n = 1000$	$n = 10000$	$n = 50000$
0.2	0.0009985	0.0005589	0.0003432	0.0003354	0.0003335	0.0003324
0.4	0.0162269	0.0090854	0.0055789	0.0054528	0.0054213	0.0054038
0.6	0.0841471	0.0472200	0.0290002	0.0283450	0.0281812	0.0280900
0.8	0.2741287	0.1548149	0.0951107	0.0929640	0.0924270	0.0921279
1.0	0.6926801	0.3961417	0.2435158	0.2380303	0.2366565	0.2358908

by a factor of 1.1659×10^{20} .

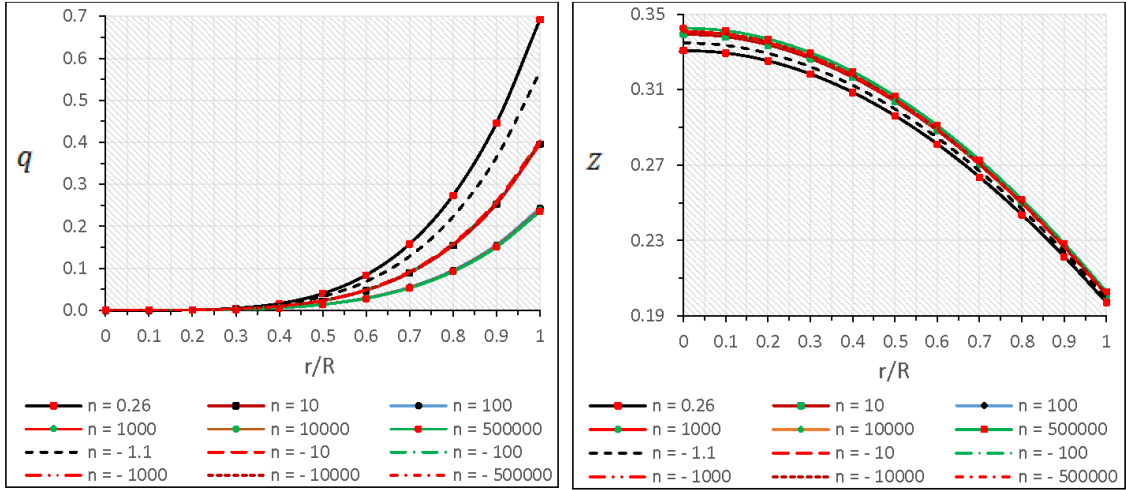


FIG. 6: (Left panel) Behavior of electric charge (q) verses fractional radius r/R for Her X-1. (Right panel) Behavior of redshift (Z) verses fractional radius r/R for Her X-1. The numerical values of the constants are given in tables 1 & 2.

F. Effective mass and compactness parameter for the charged compact star

Now we proceed with mass to radius ratio (M/R) of a relativistic compact star. Indeed, for bounds on spherically symmetric isotropic fluid sphere it is given by $2M/R \leq 8/9$, according to Buchdahl [50]. We note that for a compact charged fluid sphere there is a lower bound for the mass-radius ratio, which is [51]

$$\frac{Q^2 (18R^2 + Q^2)}{2R^2 (12R^2 + Q^2)} \leq \frac{M}{R}, \quad (41)$$

TABLE IV: The electric charge for compact star Her X-1 for different negative values of n in Km.

r/a	$n = -1.1$	$n = -10$	$n = -100$	$n = -1000$	$n = -10000$	$n = -50000$
0.2	0.0008130	0.00058101	0.0005733	0.0005724	0.0005707	0.0005691
0.4	0.0131827	0.009420316	0.0092952	0.0092802	0.0092533	0.0092265
0.6	0.0682580	0.0487584	0.0481082	0.0480300	0.0478910	0.0477524
0.8	0.2228174	0.1589667	0.1568228	0.1565654	0.1561122	0.1556601
1.0	0.5678978	0.4039877	0.3984088	0.3977420	0.3965893	0.3954407

for the constraint $Q < M$. This result was generalized by [46], for new bounds on mass-radius ratio for charged compact object with the following relation

$$\frac{M}{R} \leq \left[\frac{4R^2 + 3Q^2}{9R^2} + \frac{2}{9R} \sqrt{R^2 + 3Q^2} \right]. \quad (42)$$

Now, using the Eqs. (41) and (42), we obtain the mass-radius ratio within the entrapped region

$$\frac{Q^2 (18R^2 + Q^2)}{2R^2 (12R^2 + Q^2)} \leq \frac{M}{R} \leq \left[\frac{4R^2 + 3Q^2}{9R^2} + \frac{2}{9R} \sqrt{R^2 + 3Q^2} \right]. \quad (43)$$

To obtain the effective mass for charged fluid sphere within the radius $r=R$, one can then compute as

$$m_{\text{eff}} = 4\pi \int_0^R \left(\rho + \frac{E^2}{8\pi} \right) r^2 dr = \frac{R}{2} [1 - e^{-\lambda(R)}], \quad (44)$$

where $e^{-\lambda}$ is given by the equation Eq. (19). Following the results, the compactness factor can be written as

$$u(R) = \frac{m_{\text{eff}}(R)}{R} = \frac{1}{2} [1 - e^{-\lambda(R)}]. \quad (45)$$

Let us now consider the surface redshift, which allow us to write down the following expression as

$$Z_s = (1 - 2u)^{-\frac{1}{2}} - 1 = \sqrt{1 + D A R^2 (1 - A R^2)} - 1, \quad (46)$$

Note that for the isotropic stellar configuration the maximum possible of surface redshift is $Z_s = 4.77$, but it may be exceeded in the presence of anisotropy pressure according to [47]. In our model, this condition fall within the limit for isotropic pressure given in Table V & VI (extreme right position). The above study is carried out for both positive and negative values of n , using Eq. (46) which has been shown in Fig. 6, right panel. In Table V, the numerical method is used in this study that evident the existence for a physically viable

TABLE V: List of solution with a given range of parameters that evident the existence for a physically viable model with ansatz for metric potential (19) for compact star Her X-1.

Range of n & b	Electric charge (E)	Anisotropy Pressure (Δ)	Velocity of Sound ($dp_i/d\rho$)	List of Reference
$n, b \in \mathbb{R}^+ \cup 0$ & $n \neq -1$	$E=0$	$\Delta \neq 0$	Yes ($4 \leq n \leq 10$)	[48]
$n, b \in \mathbb{R}^- \cup 0$	$E \neq 0$	$\Delta = 0$	Yes ($n \geq 2$)	[49]
$n, b \in \mathbb{R}$	$E^2 = q_0 a^2 r^4 (1 + br^2)^{2n}$	$\Delta \neq 0$	Yes $n \in (-\infty, -1.1] \cup [0.26, \infty)$	Present Case

model with ansatz for metric potential (19) for compact star Her X-1 within a given range of parameters.

I. DISCUSSION

In this work, we have studied a class of new exact solutions with anisotropic fluid distribution of matter for compact objects in hydrostatic equilibrium. We considered the Einstein- Maxwell system with anisotropic spherically symmetric gravitating source and obtained novel gravitational solutions compatible with observational data for compact object Her X-1. We matched the interior solution to an exterior Reissner-Nordström solution, and study some physical features of the models, such as the energy conditions, speeds of sound, and mass-radius ratio. We have used the condition arising from embedding a 4-d spherically symmetric static metric in spherical coordinates into a 5-d flat space-time to model a charged object. What we employed is so-called class one space-time.

We have found that energy density, radial and tangential pressures are finite at the center, and monotonically degreasing functions with respect to the radial co-ordinate for our specific choice of generic function which is illustrated in Fig. 1 & 2, respectively. Moreover, the radial pressure vanishes at the boundary of the star, whilst the tangential one is nonvanishing at the stellar surface. We notice that the radial and tangential pressures increase with an increase of $|n|$ and energy density is maximum at the core of the star. In Table V & VI we tabulated the calculated values of central and surface density, central pressures for compact objects considering HER X-1 as an charged anisotropic star.

Our analysis shows that total charge value of a compact object to see any appreciable effect is around 10^{20} [C] and the electric fields have to be huge ($\sim 10^{20}$) in the equilibrium and stability of the star. More specifically, electric charge that produces significant effect on the structure and stability of the object, has the maximum value at the boundary of the star and monotonically increasing away from the centre. The electric charge q , against the radial coordinate has been plotted in Fig. 6 (left panel), for different parametric values of n .

We further extend our analysis by investigating the energy conditions, hydrostatic equilibrium under the different forces, and velocity of sound. We have found through our analysis that all energy conditions are satisfied at the interior of the configuration and maintain a equilibrium situation for subject to different forces due to anisotropy and electromagnetic effect as we can see observing Figs. 3 & 4. We found that when $|n|$ is small the electromagnetic force dominates the anisotropy force near and at the surface of the star, while, $|n|$ is large, the anisotropy force dominates the electromagnetic one.

Using the values given in Table 1 & 2, we check for square of the velocity of sound for anisotropic matter distribution. As illustrated in Fig. 5, our model obeys the causality throughout the stellar interior. We also pointed out that the surface red-shift has greater value in case of anisotropic star than isotropic one which is given in extreme right of Table V & VI for different values of n . Further, we show that maximum allowed masses with their respective radii i.e., mass-radius ratio fall within the limit of $8/9$ ($= 2M/R$) as proposed by Buchdahl [50], for compact objects considering HER X-1 that we have considered for our model. Finally, considering the charged stars with specific electromagnetic field can be used as a tool to prob other compact objects like HER X-1.

Acknowledgments: The author S. K. Maurya acknowledges authority of University of Nizwa for their continuous support and encouragement to carry out this research work. AB is thankful to the University of KwaZulu-Natal for financial support and Inter-University Centre for Astronomy and Astrophysics, Pune, India for providing research facilities.

- [1] R. Ruderma: *Rev. Astr. Astrophys.*, **10**, 427 (1972).
- [2] R. L. Bower and E. P.T Liang: *Astrophys. J.*, **188**, 657 (1974).

- [3] M. K. Mak and T. Harko: *Proc.Roy.Soc.Lond. A* , **459**, 393-408 (2003).
- [4] R. Sharma and S.D. Maharaj: *Mon.Not.Roy.Astron.Soc.*, **375**, 1265-1268 (2007).
- [5] F. Rahaman *et al.*: *Eur.Phys.J. C*, **72** 2071 (2012).
- [6] A. Banerjee *et al.*: *Eur.Phys.J.Plus*, **132**, 150 (2017).
- [7] D. Kileba Matondo and S.D. Maharaj: *Astrophys.Space Sci.*, **361**, 221 (2016).
- [8] B. V. Ivanov: e-Print: arXiv:1708.07971.
- [9] S. K. Maurya and S.D. Maharaj: *Eur.Phys.J. C*, **77**, 328 (2017).
- [10] Jose D. V. Arbanil and M. Malheiro: *JCAP*, **1611**, 012 (2016).
- [11] P. Bhar and B.S. Ratanpal: *Astrophys.Space Sci.*, **361**, 217 (2016).
- [12] F. Rahaman *et al.*: *Eur.Phys.J. C*, **75**, 564 (2015).
- [13] S. Hansraj: *Eur.Phys.J. C*, **77**, 557 (2017).
- [14] L. Schläfli: *Ann. di Mat. 2^e série* **5**, 170 (1871).
- [15] H. Whitney: *Ann. Math.*, **37**, 645-680 (1936).
- [16] M. Janet: *Ann. Soc. Polon. Math.*, **5**, 38 (1926).
- [17] E. Cartan: *Ann. Soc. Polon. Math.*, **6**, 1 (1927).
- [18] L. Randall and R. Sundrum: *Phys. Rev. Lett.*, **83**, 4690-4693 (1999).
- [19] R. Maartens and K. Koyama: Brane-world gravity, arXiv:1004.3962v1 [hepth].
- [20] K. R. Karmarkar: *Proc. Ind. Acad. Sci. A*, **27**, 56 (1948).
- [21] S. K. Maurya *et al.*: *Eur. Phys. J. A*, **52**, 191 (2016).
- [22] Ksh. Newton Singh, Neeraj Pant and M. Govender: *Chin.Phys. C*, **41**, 015103 (2017).
- [23] P. Bhar *et al.*: *Int.J.Mod.Phys. D*, **26**, 1750078 (2017).
- [24] S. K. Maurya, B. S. Ratanpal and M. Govender: *Annals of Physics*, **382**, 36 (2017).
- [25] K. N. Singh, N. Pant and M. Govender: *Eur. Phys. J. C*, **77**, 100 (2017).
- [26] S. K. Maurya *et al.*: *Eur. Phys. J. A*, **52**, 191 (2016).
- [27] S. K. Maurya *et al.*: *Eur. Phys. J. C*, **75**, 225 (2015).
- [28] S. K. Maurya *et al.*: *Eur. Phys. J. C* **76**, 266 (2016).
- [29] S. K. Maurya *et al.*: *Astrophys. Space Sci.*, **361**, 351 (2016).
- [30] K. N. Singh and N. Pant: *Astrophys. Space Sci.*, **361**, 177 (2016).
- [31] K. N. Singh *et al.*: *Eur. Phys. J. C*, **76**, 524 (2016).
- [32] K. N. Singh *et al.*: *Chin. Phys. C*, **41**, 015103 (2017).
- [33] Jose D. V. Arbanil and M. Malheiro: *AIP Conf.Proc.*, **1693**, 030007 (2015).

- [34] T. Gangopadhyay *et al.*: *Mon. Not. R. Astron. Soc.*, **431**, 3216 (2013).
- [35] P. Bhar *et al.*: *Eur.Phys.J. C*, **77**, 596 (2017).
- [36] S. K. Maurya and M. Govender: *Eur.Phys.J. C*, **77**, 347 (2017).
- [37] S. K. Maurya, B. S. Ratanpal and M. Govender: *Annals Phys.*, **382** 36-49 (2017).
- [38] S. K. Maurya *et al.*: *Eur. Phys. J. C*, **77**, 45 (2017).
- [39] G. Abbas, M. Zubair and G. Mustafa: *Astrophys.Space Sci.*, **26**, 358 (2015).
- [40] F. Rahaman *et al.*: *Eur.Phys.J. C*, **72**, 2071 (2012).
- [41] C. W. Misner & D. H. Sharp: *Phys. Rev. B*, **136**, 571 (1964).
- [42] R. C. Tolman: *Phys. Rev.*, **55**, 364 (1939).
- [43] J. R. Oppenheimer and G.M. Volkoff: *Phys. Rev.*, **55**, 374 (1939).
- [44] S. Ray *et al.*: *Phys Rev. D*, **68**, 084004 (2003).
- [45] J. D. Bekenstein: *Phys. Rev. D*, **4**, 2185 (1971).
- [46] H. Andréasson: *Commun. Math. Phys.*, **288**, 715 (2009).
- [47] R. L. Bowers and E. P. T. Liang: *Astrophys. J.*, **188**, 657 (1974).
- [48] P. Bhar *et al.*: *Eur. Phys. J. A* , **52**, 312 (2016).
- [49] S. K. Maurya, S. Ray, S. Ghosh, S. Manna, T. T. Smitha: *Submitted in Eur. Phys. J. C* (2017).
- [50] H. A. Buchdahl: *Phys. Rev.*, **116**, 1027 (1959).
- [51] C. G. Böhmer and T. Harko: *Class. Quantum Gravit.*, **23**, 6479 (2006).
- [52] C. Germani and R. Maartens: *Phys. Rev. D*, **64**, 124010 (2001).
- [53] L. Herrera: *Phys. Lett. A*, **165**, 206 (1992).